INTERNATIONAL JOURNAL FOR NUMERICAL METHODS IN FLUIDS
Int. J. Numer. Meth. Fluids 2000; **34**: 449–462

The discrete transfer radiation model in a natural gas-fired furnace

E. P. Keramida[a], H. H. Liakos[a], M. A. Founti[b], A. G. Boudouvis[a,*] and N. C. Markatos[a]

[a] *Department of Chemical Engineering, National Technical University of Athens, Zografou Campus, Athens 157 80, Greece*
[b] *Department of Mechanical Engineering, National Technical University of Athens, Zografou Campus, Athens 157 80, Greece*

SUMMARY

The performance of the discrete transfer radiation model is assessed in a swirling natural gas diffusion flame confined in an axisymmetric furnace. The predictions are evaluated as part of a complete prediction procedure involving the modeling of the simultaneously occurring flow, combustion, convection and radiation phenomena. Computational results with and without radiation effects are compared with experimental data and the discrete transfer model is evaluated in terms of computational efficiency, ease of application and predictive accuracy. The results have demonstrated that the effect of thermal radiation is important, even in light flames, and that the discrete transfer model can be applied in industrial gas furnaces, yielding accurate predictions. Copyright © 2000 John Wiley & Sons, Ltd.

KEY WORDS: discrete transfer model; natural gas furnaces; radiation

1. INTRODUCTION

Thermal radiation in gaseous media can be an important mode of heat transfer in high temperature chambers, such as industrial furnaces and boilers, even under non-soot conditions. Growing concern with high temperature processes has emphasized the need for an evaluation of the effect of radiative heat transfer. For example, thermal radiation affects the structure and extinction characteristics of a methane–air flame owing to the radiative cooling mechanism [1,2], as well as the nitrogen monoxide (NO) formation due to the sensitivity of thermal NO kinetics to temperature [3].

* Correspondence to: boudouvi@chemeng.ntua.gr

Copyright © 2000 John Wiley & Sons, Ltd.

Received June 1999
Revised October 1999

Nevertheless, the modeling of radiative transfer is often neglected in combustion analysis, mainly because it involves tedious mathematics, which increase the computation time, and also because of the lack of detailed information on the optical properties of the participating media and surfaces. Ignoring radiative transfer may introduce significant errors in the overall predictions. In previously published evaluations of radiation models for gaseous furnaces, the models have been tested separately, i.e., in isolation from the modeling of other physical processes, by using prescribed radiative energy source term distributions [4–11]. In real operating furnaces, non-uniform distributions of velocity and temperatures are encountered and the predictive behavior of any radiation model is expected to differ from the simplified case [4,12,13].

A numerical experiment is carried out in this paper, using the discrete transfer model to analyze the radiative heat transfer in an industrial natural gas furnace configuration. The predictions are evaluated as part of a complete prediction procedure involving the modeling of the simultaneously occurring flow, combustion, convection and radiation phenomena.

2. RADIATION MODELING

The most accurate procedures available for computing radiation transfer in furnaces are the zone [14] and the Monte Carlo [15] methods. However, these methods are not widely applied in comprehensive combustion calculations due to their large computational time and storage requirements. Also, the equations of the radiation transfer are in non-differential form—a significant inconvenience when solved simultaneously with the differential equations of flow and combustion.

For industrial furnace applications, radiation modeling is directed towards more efficient but less fundamental flux methods (see Reference [16] for an extensive review). Efficiency becomes particularly important in the development of combustion codes, where the flow, combustion and heat transfer are computed simultaneously. Radiation models should be realistic enough to yield meaningful results but also simple enough to overcome the associated numerical difficulties.

Shah's discrete transfer radiation model [6], which combines features of the zone, Monte Carlo and flux models, is applied here to a benchmark combustion case.

With the discrete transfer model, the total radiative flux is calculated by integrating the energy contribution along rays emanating from the radiative source and pointing to any selected direction. The discrete transfer model

(a) retains the physics of the problem with relatively simple mathematics;
(b) has the ability to return any desired degree of precision by increasing the number of rays projected from each physical surface and the number of zones that the domain is divided into; however, this adds considerably to the cost of computation;
(c) it requires a surface model to describe the geometry;
(d) may require carefully shaped control volumes and positioning of the rays to yield accurate predictions;
(e) requires Cartesian co-ordinates.

Copyright © 2000 John Wiley & Sons, Ltd.

3. THE PHYSICAL AND MATHEMATICAL MODEL

3.1. Furnace configuration

The benchmark case studied is a typical chamber of gaseous combustion, the so-called 'Harwell furnace', which is a cylindrical enclosure of 0.15 m in radius and 0.9 m in length [17,18]. Two reactant streams emerge from two separate coaxial jets producing a swirling diffusion flame. The fuel is injected from the central jet whereas the combustion air enters from the outer annular jet. The geometry of this natural gas furnace is illustrated in Figure 1 and the inlet conditions for the fuel and air are shown in Table I.

3.2. Mathematical model

A two-dimensional mathematical model is developed simulating the flow and chemical reaction in the combustion chamber. The model consists of the partial differential equations (PDEs) describing the conservation of momentum, heat-transfer and mass species, in conjunction with a two-equation turbulence model. The equations are expressed, for each variable, in a generalized form as

$$\frac{\partial}{\partial t}(\rho\Phi) + \operatorname{div}(\rho\underline{u}\Phi - \Gamma_\Phi \operatorname{grad}\Phi) = S_\Phi \tag{1}$$

where Φ is any of n variables [19], Γ_Φ is the diffusion coefficient and S_Φ is the source term of the variable Φ. The turbulent stress terms that enter the equations of turbulent kinetic energy and of the dissipation of turbulence are calculated with the standard $k-\varepsilon$ model of turbulence [20].

As far as the combustion modeling is concerned, widely applied combustion models like the eddy break-up (EBU) [21] or the eddy dissipation concept model [22], have the following limitations: (a) reaction rate does not depend on local chemistry, and (b) the transport of the turbulent flame by the flow is not described. That is why a more advanced combustion model has been used in this work; it is an extension of the eddy break-up model, by Mantel and

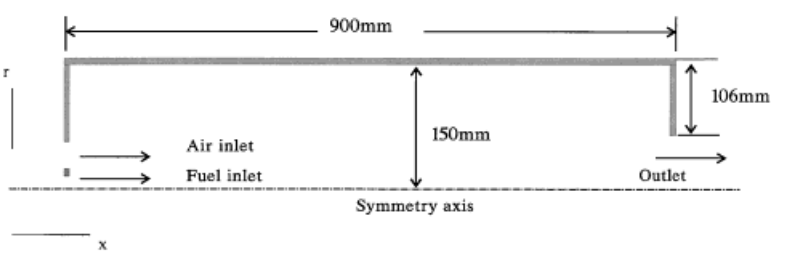

Figure 1. Geometry of the combustion chamber.

Copyright © 2000 John Wiley & Sons, Ltd.

Table I. Input conditions and fluid properties.

Geometry		
Fuel inlet zone (mm)	from $r = 0.0$	to $r = 6.0$
Air inlet zone (mm)	from $r = 16.5$	to $r = 27.5$
Furnace diameter (mm)	150.0	
Furnace length (mm)	900.0	
Inlet boundary conditions	**Fuel**	**Air**
Axial velocity	15.0	12.8
Radial velocity	0.0	0.0
Turbulent kinetic energy	2.26	1.63
Dissipation rate of turbulence	1131.8	692.0
Temperature	295	295
Swirl number	0.0	0.4
Composition (mass fraction)	**Fuel**	**Air**
O_2	0.0	0.2315
N_2	0.0	0.7685
CH_4	1.0	0.0
Heat of reaction (MJ kg^{-1})	45.5	

Borghi [23], as formulated below. The use of this model is recommended for flames with high Damkohler and high turbulent Reynolds numbers, like in the present case. This model takes into account the interaction between the chemistry and the turbulence through the ratio u'/U_L. The mean reaction rate is given by the following equation:

$$\bar{w} = \rho C_{EBU} \frac{\bar{Y}(Y_0 - \bar{Y})}{\tau_t} \tag{2}$$

where

$$C_{EBU} = \frac{\alpha_0}{\beta_0} \frac{\left(1 + c\dfrac{U_L}{u'}\right)^{2\gamma}}{Y_0\left(\dfrac{1}{2} - b_0\right)} \tag{3}$$

$\bar{Y}$ is the local fuel mass fraction and Y_0 is the fuel mass fraction in the fresh mixture, ρ is the gas density, $\tau_t = k/\varepsilon$ is the eddy time scale, $u' = (\frac{2}{3}k)^{1/2}$ is the velocity fluctuation, $\alpha_0 = 0.9$, $\beta_0 = 1.25$, $b_0 = 0.2$, $c = 1.0$ and $\gamma = 1.0$ are model constants. The laminar burning velocity is taken $U_L = 0.34$ m s^{-1} [24] for stoichiometric methane–air mixtures at atmospheric conditions. The turbulent burning velocity is calculated from the following equation:

Copyright © 2000 John Wiley & Sons, Ltd.

$$U_T = (U_L + 2.25u')^{1/2} \tag{4}$$

The combustion gas is taken as a mixture of oxygen, nitrogen, carbon dioxide, water vapor and fuel gas. The gas temperature is derived from the enthalpy equation, where the specific heat is calculated as the weighted sum of the individual specific heat of the mixture components. The gas density is evaluated from the ideal gas equation of state.

3.3. The discrete transfer model

The basis of all methods for the solution of radiation problems is the radiative transfer equation (RTE)

$$\underline{s} \cdot \nabla I(\underline{r}, \underline{s}) = -\kappa(\underline{r}) I(\underline{r}, \underline{s}) + Q(\underline{r}, \underline{s}) \tag{5}$$

which describes the radiative intensity field, I, within the enclosure, as a function of location vector ($\underline{r}$) and direction vector ($\underline{s}$); Q represents the total attenuation of the radiative intensity due to the gas emission and to the in-scattered energy from other directions to the direction of propagation, and κ is the total extinction coefficient.

The discrete transfer model discretizes the RTE along rays. The path along a ray is discretized by using the sections formed from breaking the path at zone boundaries. Assuming that the physical properties remain constant inside a zone, Equation (5) can be integrated from zone entry to zone exit (Figure 2) to yield

$$I_{n+1} = I_n \, e^{-\tau_n} + L_n Q_n \left[\frac{1 - e^{\tau_n}}{\tau_n} \right], \quad \tau_n = \kappa L_n \tag{6}$$

where L_n is the path length in the nth zone, I_n and I_{n+1} are the intensities at zone entry and zone exit respectively, and

$$Q_n(\underline{r}, \underline{s}) = \frac{k_a}{\pi} \sigma T_n^4 + k_s J_n(\underline{r}) \tag{7}$$

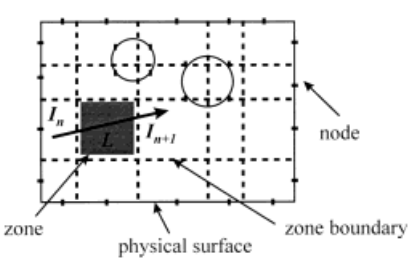

Figure 2. Sub-division of the solution domain into zones.

Copyright © 2000 John Wiley & Sons, Ltd.

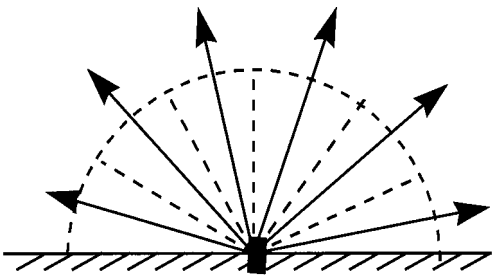

Figure 3. Projection of a ray at a node into a number of angular volumes.

where k_a, k_s are the absorption and scattering coefficients for a gray medium, $J_n(\underline{r}) = (1/4\pi)\int I_n(\underline{r}, \underline{s})\,d\Omega$ is the mean intensity of the in-scattered radiation, σ is the Stefan–Boltzmann constant and $d\Omega$ is the element of solid angle containing $\underline{s}$.

The rays are chosen by fixing nodes to all the physical surfaces, dividing up the interior hemisphere into elements of equal solid angle and projecting one ray into each solid angle (Figure 3).

For gray surfaces, integration of Equation (5) yields the required boundary conditions

$$I(\underline{r}, \underline{s}) = \frac{e_w}{\pi}\sigma T^4(\underline{r}) + \frac{1 - e_w}{\pi} R(\underline{r}) \tag{8}$$

where e_w is the wall emissivity and $R(\underline{r}) = \int_{\underline{s}\cdot\underline{n}<0} (\underline{s}\cdot\underline{n}) I(\underline{r}, \underline{s})\,d\Omega$ is the radiation flux on a surface, and $\underline{n}$ is the inward pointing unit vector normal to the surface at $\underline{r}$.

4. COMPUTATIONAL DETAILS

As already mentioned, the discrete transfer model may yield any desired degree of precision by increasing the number of rays and the number of zones. Results with various numbers of rays have been obtained demonstrating that 32 rays suffice for accurate predictions.

Another characteristic of the discrete transfer model is that it uses its own geometrical description, based on surface modeling, and is always built in Cartesian co-ordinates (flow geometry may still be in polar co-ordinates). The construction of the radiation geometry for the discrete transfer model may require carefully shaped control volumes (zones) and positioning of the rays to achieve the required solution. For example, in large systems the spatial resolution (number of zones) is normally much less than that used by the flow solver. This mainly affects the cooling rate, which is proportional to the fourth power of the temperature and can thus change by several orders of magnitude across a flame front. Large local errors occur if large opacity gradients remain unresolved by the radiation model [25]. In the case studied, different zone constructions produced different results. Crude or careless 'zoning' of the heat source (flame) will result in inaccurate average values of the temperature per zone and,

Copyright © 2000 John Wiley & Sons, Ltd.

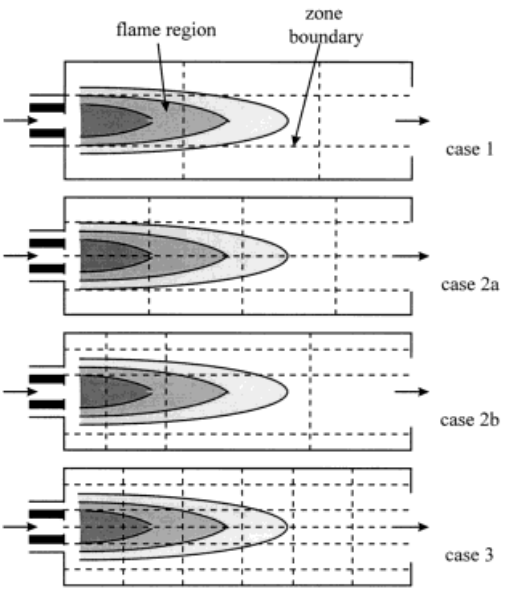

Figure 4. Hypothetical zone constructions, showing different sampling of the flame.

consequently, to inaccurate radiation calculations. In Figure 4, case (1) is an example of crude zoning, while case (3) is an example of more careful zoning, which takes into account the steep temperature variation from zone to zone. Another important issue when 'zoning' the heat sources is to ensure symmetry; comparison between case (2a) and (2b) in Figure 4 shows the difference.

The resulting system of the PDEs, along with the boundary and inlet conditions, have been solved for the various dependent variables in their two-dimensional form using polar co-ordinates and an iterative procedure, based on a staggered grid arrangement, using the SIMPLEST algorithm, the quadratic upwind differencing discretization scheme and the tri-diagonal matrix algorithm.

The solution domain was tessellated into 149 grid nodes in the axial direction and 66 grid nodes in the radial direction. Absorption and scattering coefficients used in the radiation model were taken 0.5 m^{-1} and 0.01 m^{-1} respectively [17]. The walls were treated as a gray heat sink of emissivity 0.8 and assumed to be completely water-cooled at a temperature of 400 K [17].

5. RESULTS

Comparisons between the experimental data reported by Wilkes *et al.* [17] and the calculated results obtained with and without radiation are shown in Figures 5–9. The variation of

Copyright © 2000 John Wiley & Sons, Ltd.

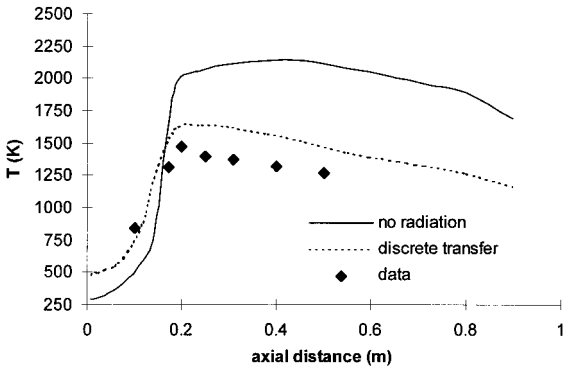

Figure 5. Mean temperature centerline along the profile (experimental data taken from Reference [17]).

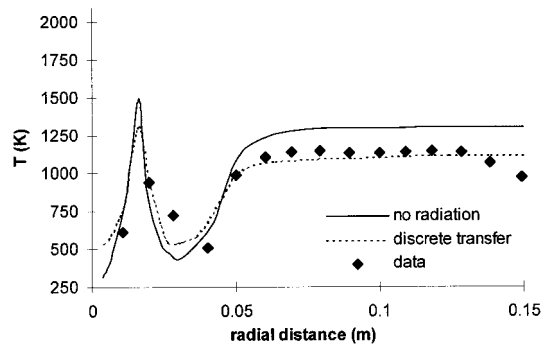

Figure 6. Radial temperature profiles at distance 0.04 m from entrance (experimental data taken from Reference [17]).

temperature along the furnace centerline is presented in Figure 5. Radial profiles of the temperature are shown at four consecutive axial locations in Figures 6–9; two near the inlets and two near the middle of the furnace. It is shown that accounting for radiation in the computational analysis has improved the accuracy of the predictions.

The reduction of the mean temperature in the furnace is significant and is more pronounced in the upstream direction, towards the furnace outlet. Close to the furnace inlets, on the other hand, increased temperature is predicted. This shows that the reactant mixture heating effect, due to the flame backward radiation, is better represented when radiation heat transfer is taken into account (Figure 5). Similar observations can be made from the radial temperature profiles shown in Figures 6 and 7. In the main combustion zone, where higher temperatures are reached, the effects of radiation are more pronounced and extend all over the furnace diameter (see Figures 8 and 9).

Copyright © 2000 John Wiley & Sons, Ltd.

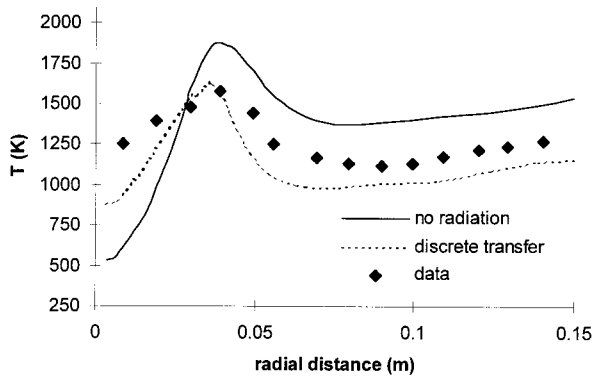

Figure 7. Radial temperature profiles at distance 0.1 m from entrance (experimental data taken from Reference [17]).

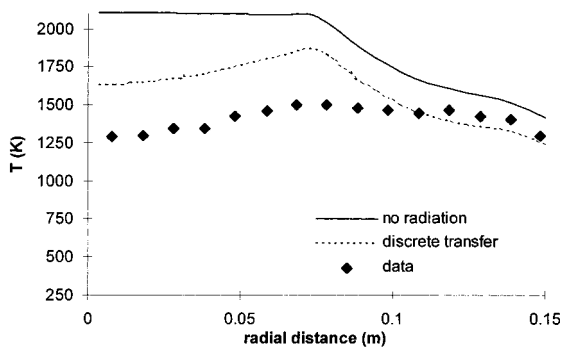

Figure 8. Radial temperature profiles at distance 0.2 m from entrance (experimental data taken from Reference [17]).

Effects of radiation are overestimated in the main zone of combustion, as shown in Figures 8 and 9. This is explained by the fact that the absorption and scattering coefficients of the participating medium, in the furnace, are assumed to be uniform. In reality, the gas composition in the main zone of combustion is highly non-uniform, consisting of fuel, oxidant and combustion products. This local increase in the gas emissivity is not accounted for in the model. As a result, the cooling rate in this particular area of the furnace is underestimated and, consequently, the temperature is overestimated.

Despite the fact that the overall heat released is the same in all the examined cases, radiative heat transfer is responsible for reducing the size the high temperature regions of the flame and for shifting them towards the furnace inlet, as it is shown by the temperature contours in Figure 10. As a result, more heat is released close to the burner when radiation is taken into

Copyright © 2000 John Wiley & Sons, Ltd.

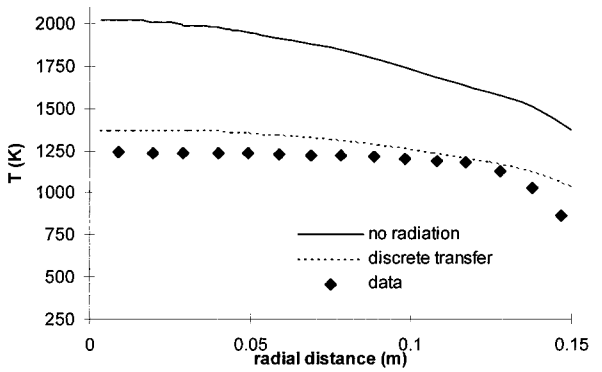

Figure 9. Radial temperature profiles at distance 0.4 m from entrance (experimental data taken from Reference [17]).

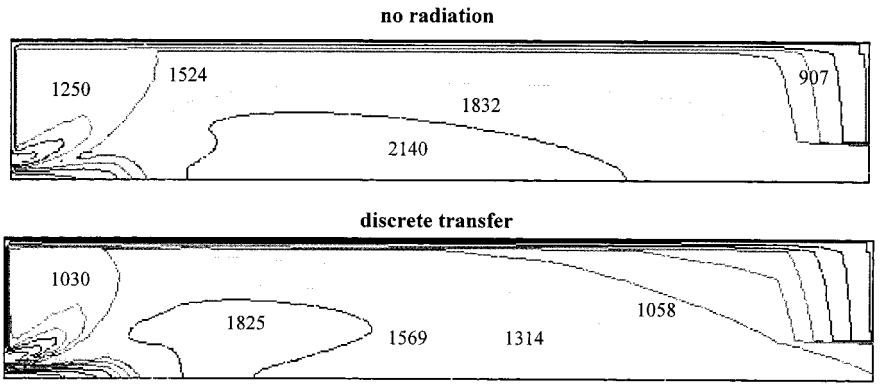

Figure 10. Contours of constant temperature.

account, resulting in steeper temperature gradients towards the furnace outlet. The combustion gases leave the furnace with nearly 60% lower temperature. This reduction of the gas enthalpy content at the outlet is counter-balanced by the increase of the total heat flux across the axial wall of the furnace.

Figure 11 shows the variation of the heat flux along the furnace axial wall. Absolute wall heat flux values are significantly increased when radiation is taken into account. The main combustion zone temperatures around the central part of the furnace do not seem to directly affect the heat losses from the wall. When radiation is taken into account, the total heat flux from the furnace wall is due to the sum of contributions of the convective and radiative heat transfer. The axial location of the maximum wall heat-flux value is shifted downstream, where maximum temperatures are encountered in the main combustion zone of the furnace. The total heat leaving through the axial wall of the system has increased about four times.

Copyright © 2000 John Wiley & Sons, Ltd.

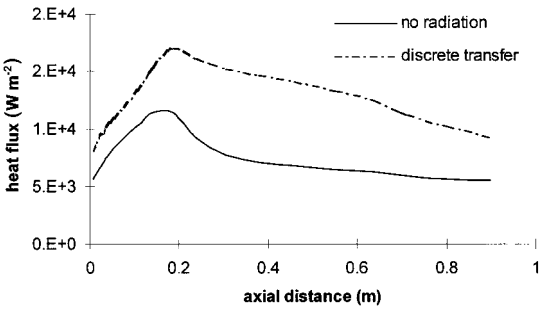

Figure 11. Heat flux distribution along the axial furnace wall (experimental data taken from Reference [17]).

6. CONCLUSIONS

There is a difference between evaluating radiation models as part of an overall predictive scheme and evaluating them independently, as the coupled effects of different interplaying processes may often reveal new evidence as to the accuracy of the models. The present work attempts to examine numerically a turbulent, non-premixed natural gas flame with and without consideration of the radiation effects. The discrete transfer model has been used for this purpose.

The results have confirmed that the effect of thermal radiation is important on flame temperature predictions. The inclusion of radiative heat transfer in the combustion analysis has produced a better agreement between numerical predictions and experimental data. It has resulted in an increase of the levels of computed temperatures near the reactants inlet, and to a substantial decrease in the main combustion zone, near the walls and the exit of the furnace. These observations indicate that computations involving only convective heat transfer mechanisms underpredict the heating effect of the reactants mixture at the inlet, and overpredict the temperature levels everywhere else.

The inclusion of thermal radiation in the analysis has also reduced the size of the flame region where maximum temperatures are located. Finally, it has increased by about four times the percentage of heat leaving through the axis wall of the system, emphasizing the significance of this particular sink term in the total enthalpy balance.

As far as the evaluation of the discrete transfer radiation model is concerned, in the present work the model yields reasonable accuracy. The discrete transfer model can be recommended for simplified heat transfer analysis in combustion systems, as it is a relatively simple model, regarding mathematics and implementation effort. The only disadvantage of the model is its geometry description requirements; it may prove tricky in terms of dividing the domain into zones to construct an adequate radiation geometry. Finally, the discrete transfer has proved an expensive model, regarding computational cost.

In the course of further improving the quantitative prediction of the model, account should be taken of the variation in the optical properties of the participating combustion gases.

Copyright © 2000 John Wiley & Sons, Ltd.

APPENDIX A. NOMENCLATURE

a_0	constant used in the reaction model
b_0	constant used in the reaction model
c	constant used in the reaction model
C_{EBU}	variable in the reaction model
e_{w}	surface emissivity
E	emissive power ($\mathrm{W\,m^{-2}}$)
I	radiative intensity ($\mathrm{W\,m^{-2}\,r^{-1}}$)
J	mean intensity of the in-scattered radiation ($\mathrm{W\,m^{-2}\,r^{-1}}$)
k	turbulence kinetic energy ($\mathrm{m^2\,s^{-2}}$)
k_{a}	gas absorption coefficient ($\mathrm{m^{-1}}$)
k_{s}	gas scattering coefficient ($\mathrm{m^{-1}}$)
L	path length (m)
Q	total attenuation of the radiative intensity due to emission and in-scattering ($\mathrm{W\,m^{-2}}$)
$\underline{r}$	direction vector
R	radiation flux ($\mathrm{W\,m^{-2}}$)
$\underline{s}$	location vector
S_Φ	source term
t	time (s)
τ_{t}	eddy time scale (s)
T	temperature (K)
$\underline{u}$	velocity ($\mathrm{m\,s^{-1}}$)
u'	velocity's fluctuation ($\mathrm{m\,s^{-1}}$)
U_{L}	laminar burning velocity ($\mathrm{m\,s^{-1}}$)
U_{T}	turbulent burning velocity ($\mathrm{m\,s^{-1}}$)
$\bar{w}$	mean reaction rate ($\mathrm{kg\,m^{-3}\,s^{-1}}$)
x, r	co-ordinate axes in cylindrical geometry
$\bar{Y}$	fuel mass fraction
Y_0	fuel mass fraction in the fresh mixture

Greek letters

α_0	constant used in the reaction model
β_0	constant used in the reaction model
ε	dissipation rate of turbulence ($\mathrm{m^2\,s^{-3}}$)
γ	constant used in the reaction model
κ	extinction coefficient ($\mathrm{m^{-1}}$)
μ	viscosity ($\mathrm{kg\,m^{-1}\,s^{-1}}$)
ρ	density ($\mathrm{kg\,m^{-3}}$)
σ	Stefan–Boltzmann constant, 5.67×10^{-8} ($\mathrm{W\,m^{-2}\,K^{-4}}$)

Copyright © 2000 John Wiley & Sons, Ltd.

τ	optical thickness
Φ	transport variable
Γ_Φ	diffusion coefficient
Ω	solid angle (sr)

Subscripts

n	zone number
w	wall

REFERENCES

1. Guo H, Ju Y, Maura K, Niioka T. Radiation extinction limit of counterflow premixed lean methane-air flames. *Combustion and Flame* 1997; **109**: 639–646.
2. Abbud-Madrid A, Ronney DP. Effects of radiative and diffusive transport processes on premixed flames near flammability limits. In *Proceedings of the 23rd Symposium (International) on Combustion*. The Combustion Institute: Pittsburgh, PA, 1990; 423–431.
3. Chan SH, Pan XC, Abou-Ellail MMM. Flamelet structure of radiating CH_4–air flames. *Combustion and Flame* 1995; **102**: 438–446.
4. Jamaluddin AS, Smith PJ. Predicting radiative transfer in axisymmetric cylindrical enclosures using the discrete ordinates method. *Combustion Science and Technology* 1988; **62**: 173–186.
5. Selcuk N. Evaluation for radiative transfer in rectangular furnaces. *International Journal for Heat and Mass Transfer* 1988; **31**: 1477–1482.
6. Lockwood FC, Shah NG. A new radiation solution method for incorporation in general combustion prediction procedures. In *Proceedings of the 18th Symposium (International) on Combustion*. The Combustion Institute: Pittsburgh, PA, 1981; 1405–1416.
7. Ratzell AC, Howell JR. Two-dimensional radiation in absorbing-emitting media using the P–N approximation. *ASME Journal of Heat Transfer* 1983; **105**: 333–340.
8. Siddall RG. Flux methods for the analysis of radiant heat transfer. *Journal of the Institute of Fuel* 1974; **101**: 101–109.
9. Selcuk N, Kayakol N. Evaluation of discrete ordinates method for radiative transfer in rectangular furnaces. *International Journal of Heat and Mass Transfer* 1997; **40**: 213–222.
10. Liu F, Becker HA, Bindar Y. A comparative study of radiative heat transfer modelling in gas-fired furnaces using the simple grey gas and the weighted-sum-of-grey-gases models. *International Journal of Heat and Mass Transfer* 1998; **41**: 3357–3371.
11. Wieringa JA, Elich JJ, Hoogendoorn CJ. Spectral effects of radiative heat transfer in high-temperature furnaces burning natural gas. *Journal of the Institute of Energy* 1990; **LXIII**(456): 101–108.
12. Doherty P, Fairweather M. Predictions of the radiative transfer from non-homogenous combustion products using the discrete transfer method. *Combustion and Flame* 1988; **71**(1): 79–87.
13. Varnas SR, Truelove JS. Simulating radiative transfer in flash smelting furnaces. *Applied Mathematical Modelling* 1995; **19**: 456–464.
14. Hottel HC, Sarofim AF. The effect of gas flow patterns on radiative transfer in cylindrical furnaces. *International Journal of Heat and Mass Transfer* 1965; **8**: 1153–1169.
15. Steward FR, Cannon P. The calculation of radiative heat flux in a cylindrical furnace using the Monte Carlo method. *International Journal of Heat and Mass Transfer* 1971; **14**: 245–262.
16. Douglas Smoot L. Pulverized coal diffusion flames: a perspective through modeling. In *Proceedings of the 18th Symposium (International) on Combustion*. The Combustion Institute: Pittsburgh, PA, 1981; 1185–1202.
17. Wilkes NS, Guilbert PW, Shepherd CM, Simcox S. The application of HARWELL–FLOW3D to combustion models. AERE-R13508, Atomic Energy Authority Report, Harwell, UK, 1989.
18. Truelove JS. Evaluation of a multi-flux model for radiative heat transfer in cylindrical furnaces. AERE-R9100, Atomic Energy Authority Report, Harwell, UK, 1978.
19. Markatos NC, Cox G. Hydrodynamics and heat transfer in enclosures containing a fire source. *Physicochemical Hydrodynamics* 1984; **5**: 53–65.

Copyright © 2000 John Wiley & Sons, Ltd.

20. Launder BE, Spalding DB. The numerical computation of turbulent flows. *Computing Methods in Applied Mechanics and Engineering* 1974; **3**: 269–289.
21. Spalding DB. Development of the eddy break-up model of turbulent combustion. In *Proceedings of the 16th Symposium (International) on Combustion*. The Combustion Institute: Pittsburgh, PA, 1977; 1657–1663.
22. Magnussen BF, Hjertager BH. On the mathematical modeling of turbulent combustion with special emphasis on soot formation and combustion. In *Proceedings of the 16th Symposium (International) on Combustion*. The Combustion Institute: Pittsburgh, PA, 1976; 719–730.
23. Mantel T, Borghi R. A new model of premixed wrinkled flame propagation based on a scalar dissipation equation. *Combustion and Flame* 1994; **96**: 443–457.
24. Borman GL, Ragland KW. *Combustion Engineering*. McGraw-Hill: New York, 1998.
25. Keramida EP, Karayannis AN, Boudouvis AG, Markatos NC. Radiative heat transfer in fire modeling. BFRL-NIST Annual Conference on Fire Research, NISTIR 6242, Gaithersburg, USA, 1998; 147–149.

Copyright © 2000 John Wiley & Sons, Ltd.